

## **Measurement of Impervious Surface Area from Landsat Thematic Mapper Data using Spectral Mixture Analysis**

Eugene W. Martin - eugene@commenspace.org  
The Community and Environment Spatial Analysis Center -  
www.commenspace.org  
1305 4th Ave. #1000 Seattle WA, 98101 - 206 749 0112

March, 2000

### *Acknowledgements:*

This research was made possible by a grant from the Northwest Fund for the Environment ([www.nwfund.org](http://www.nwfund.org)). Access to ArcView GIS 3.1, Spatial Analyst 1.1 and Image Analyst 1.0 provided by the Environmental Systems Research Institute Conservation Program ([www.esri.com/conservation/conservation.html](http://www.esri.com/conservation/conservation.html)). Access to Impact Spectral Mixing Analysis Software provided by the Geological Remote Sensing Laboratory at the University of Washington ([dana.geology.washington.edu](http://dana.geology.washington.edu)). Marina Alberti, Miles Logsdon, and Frank Westerlund provided thoughtful comments and reactions on this approach to impervious surface detection. Special thanks to Robin Weeks for his guidance and suggestions during the execution of this research.

### *Abstract:*

Impervious surface created by road construction, development and urbanization is an important factor influencing the health of downstream aquatic habitats (Booth, 1991, Booth and Reinelt, 1993). Impervious surfaces increase volume and 'flash' in downstream runoff events resulting in modified channel structure, increased water temperatures, reduced biodiversity and decreased water quality (Schuler, 1994). Advances in remote sensing analysis methods permit sub-pixel quantification of primary image elements using spectral mixing analysis (SMA) (Adams et al., 1986, 1993; Smith et al., 1990a,b; Gillespie et al., 1990). SMA was applied to a Landsat Thematic-Mapper (TM) image from August 1998 of Washington State's Puget Sound region to quantify pervious, semi-pervious and impervious surfaces in the Cedar River watershed subbasins. SMA endmember fraction images were used to map pixel content percents for forest canopy, open green vegetation, bare soil, dry grass and impervious surface. Results were corroborated by comparing proximity

and area of impervious surface with street and building digital geographic data. Analysis results were an important contribution to the Muckleshoot Indian Tribe's Chinook Recovery Plan.

*Introduction:*

Impervious surface created by road construction, development and urbanization is an important factor influencing the health of downstream aquatic habitats (Booth, 1991, Booth and Reinelt, 1993). Impervious surfaces increase the frequency and intensity of downstream runoff events resulting in modified channel structure, increased water temperatures, reduced biodiversity and decreased water quality (Schuler, 1994). These effects have important ecological and economic repercussions considering the benefits, services and aesthetic value provided by aquatic systems. Wetlands and riparian zones provide valuable containment and water quality mitigation services and provide important habitat for a wide variety of species. In the northwest United States, stream habitat quality is of particular importance to salmon.

The extent and spatial distribution of impervious surface relative to streams and watersheds is an important empirical measure for evaluating stream health and for making effective watershed management decisions. Impervious surface effects upon water quality and channel stability have been shown to occur when 10 – 15% of the watershed surface is impervious (Shaver et al. 1994, Booth and Reinelt, 1993). Increases in water temperature in urban streams has direct positive correlation with watershed imperviousness (Galli, 1991).

Remote sensing techniques have the potential to provide effective information resources to quantify impervious surface across a region or watershed. Aircraft and satellite borne multispectral sensors are capable of recording high resolution images from narrow bands of the visible and infrared electromagnetic spectrums. Processing techniques for these images are commonly used to derive land cover maps and assess the spatial distribution of landscape processes. The success of these efforts is a combination of potential information contained in raw image data, application of analysis techniques to extract and refine the information and knowledge of how the results contribute to understanding the phenomenon in question. While many remotely sensed land cover information products exist, they often lack the spatial and categorical detail required to support the accurate assessment of impervious area. This paper presents the results of a spectral mixture analysis applied (SMA) to a Landsat Thematic Mapper (TM) image for the purpose of quantifying impervious surface in the Cedar River watershed of Washington state. A brief introduction to the technique and its suitability for analysis of

impervious surface is provided for readers unfamiliar with SMA. Subsequent sections outline the selection of image endmembers, application of three mixing models, integration of the resulting endmember fractions and post processing analysis. The two methods used to test and verify the validity of the impervious fraction image are presented followed by a discussion of directions for improvements.

### *Spectral Mixing Analysis and Impervious Surfaces:*

SMA is a physically based image analysis process that supports repeatable and accurate extraction of quantitative sub-pixel information (Adams et al., 1986; 1993; Smith et al., 1990a). This analysis process presumes that the spectral variability in a multispectral image can be modeled by mixtures of a small number of surface materials with distinct reflectance spectra (endmembers) (Adams et al., 1989). Unlike supervised and unsupervised image classification, SMA does not rely on the detection or identification of pixel clusters with similar reflectance spectra, rather it considers each pixel individually and assesses the presence and proportion of select endmembers. SMA produces fraction images that are pixel by pixel measures of the percent composition for each endmember in the spectral mixing model. Fraction images produced with SMA have been shown to be effective in mapping natural environments (Smith et al., 1990a; Allen and Walsh, 1996; Wessman et al., 1997; Cochrane and Souza 1998), as inputs for land use change analyses (Smith et al., 1990b; 1993; Sabol et al., 1993; Sabol, 1995; Adams et al., 1995) and are suitable inputs for ecological models (Ustin et al., 1993).

The difficulty in applying SMA to disturbed, developed or urban landscapes is the variety, heterogeneity and distribution of image components that might be suitable endmembers. There is a great variety in the spectral reflectance of materials in rooftops, parking lots, streets, and sidewalks, all of which are impervious. As SMA operates on a limited set of endmembers that contribute to the spectral composition of individual pixels, there is no room for all the spectra of urban environments in the mixture model. Towards resolving this difficulty, this research focused on the integration of three different mixture models: rural/forest/agriculture/, low/mid density developed and high density developed. The variability of urban surfaces was treated with two endmembers that served as proxies for impervious surfaces.

### *Source Multispectral Image:*

The image source for this analysis was a Landsat Thematic Mapper (TM) image taken on August 27, 1998. A clip of the image encompassing the Cedar River watershed was selected for analysis. The clip extends east to west from Bainbridge

Island (Longitude: -122.645) to the Cascade Crest at Snoqualmie Pass (Longitude: -121.388) and north to south from Tacoma (Latitude: 47.2491) to Mukilteo (Latitude: 47.9377). Only the visible and infrared bands (1, 2, 3, 4, 5, & 7) of the image were used. Dark object subtraction was the only correction applied to the image.

Endmember sample locations:



*Endmember Selection:*

Image endmembers representing known components of the image clip were selected using an iterative testing process with SMA. The image clip was repeatedly analyzed with SMA using different combinations of prospective endmembers to compare their ability to model image variability. All image endmember tests included a shade proxy where values for all six bands were set to zero. Use of the shade endmember serves to normalize the analysis for differences in texture and illumination across the image. The effects of atmosphere across such a small analysis area were considered to be uniform and embedded within the spectra of the image endmembers. Prospective endmember performance was compared through scatter plots of the resulting fraction images along with the root-mean-square (RMS) values from each mixture. Six endmembers were selected for use in the three

analysis models based on their ability to distinguish desired features in the image, participation in mixtures with other endmembers and spectral distinction from other endmembers.

*Shade Proxy* – all band values assigned to zero

*Green Vegetation* – a bright green open vegetation pixel from an agricultural zone

*Impervious 1* – a bright cement pixel that produced high endmember fraction values across urban core areas

*Impervious 2* – a very bright rooftop material that had a clustered distribution in the urban core.

*Bare Soil* – tilled field

*Dry Grass* – desiccated agriculture

Table 1: Digital number values for image endmembers by TM bands

Endmember	Band1 DN	Band2 DN	Band3 DN	Band4 DN	Band5 DN	Band7 D
Shade Proxy	0	0	0	0	0	0
Green Veg.	34	18	23	158	85	22
Impervious 1	157	98	165	132	190	97
Impervious 2	227	245	255	254	255	255
Bare Soil	79	51	99	94	177	104
Dry Grass	41	24	45	72	150	55

### *Three Mixture Models:*

The process of identifying image endmembers for analysis also suggested potential combinations of endmembers to treat different land use or cover types found in the image. Spectral unmixing was performed on the image clip using the following three endmember models:

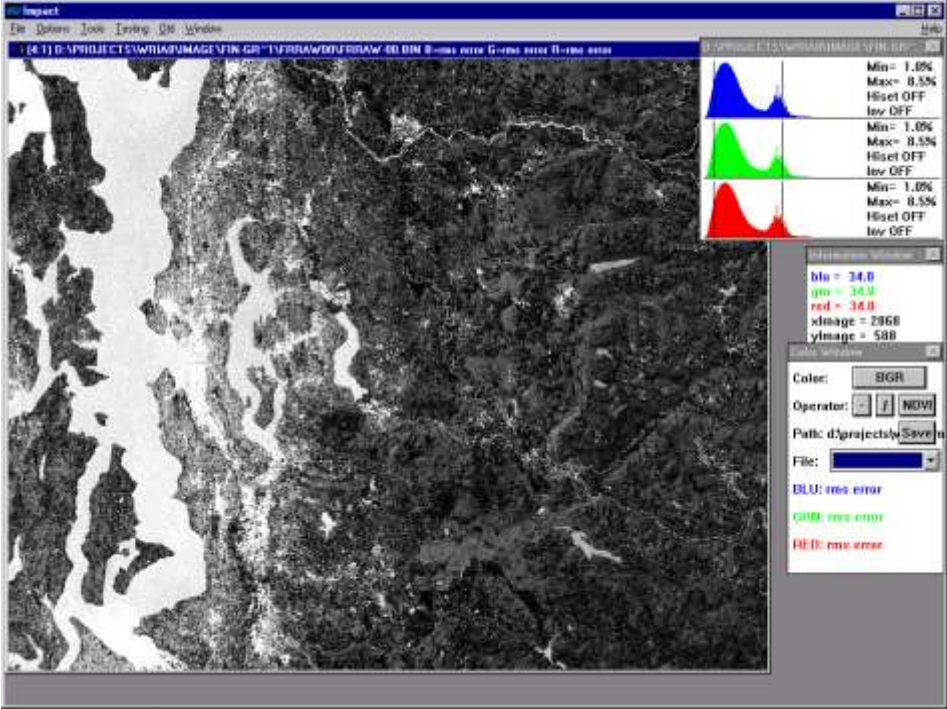
Rural/Forest/Agriculture: Green Vegetation, Bare Soil, Dry Grass, Shade

Low/Mid Density Developed: Green Vegetation, Impervious 1, Dry Grass, Shade

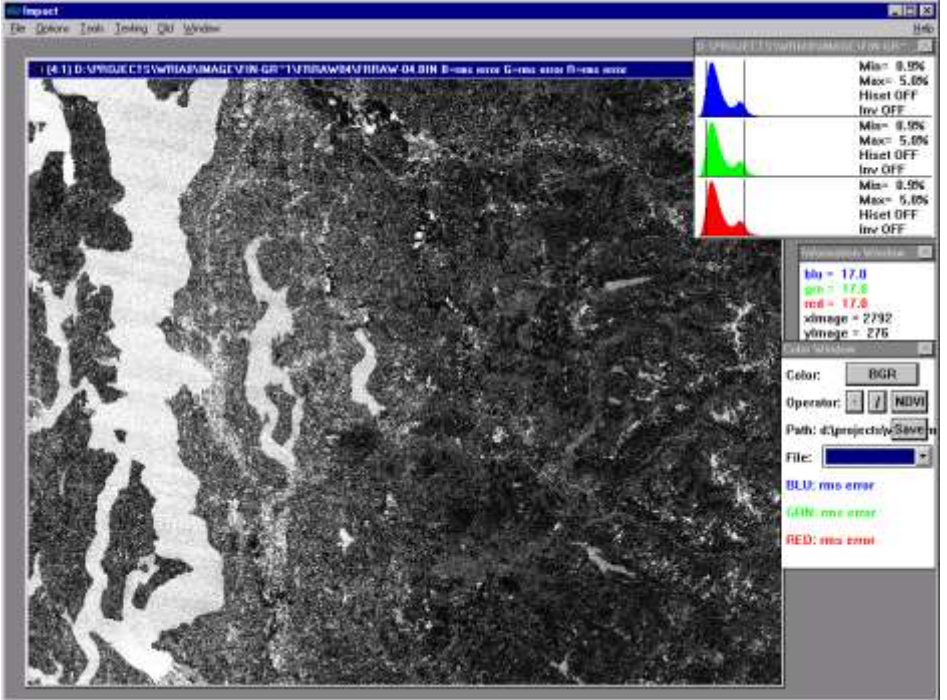
High Density Developed: Green Vegetation, Impervious 1, Impervious 2, Shade

Spectral unmixing of the image produced RMS values across all pixels of 3.3, 3.8 and 5.3 respectively for each of the three models listed above. While the RMS values for the Rural/Forest/Agriculture and Low/Mid Density Developed indicate a "good" fit across the image (RMS approaches instrument noise), pixels in the urban core of Seattle had much higher RMS values. This pattern can be seen in the fraction images for RMS where the brighter pixels indicate higher RMS values.

Rural/Forest/Agriculture model RMS fraction image.



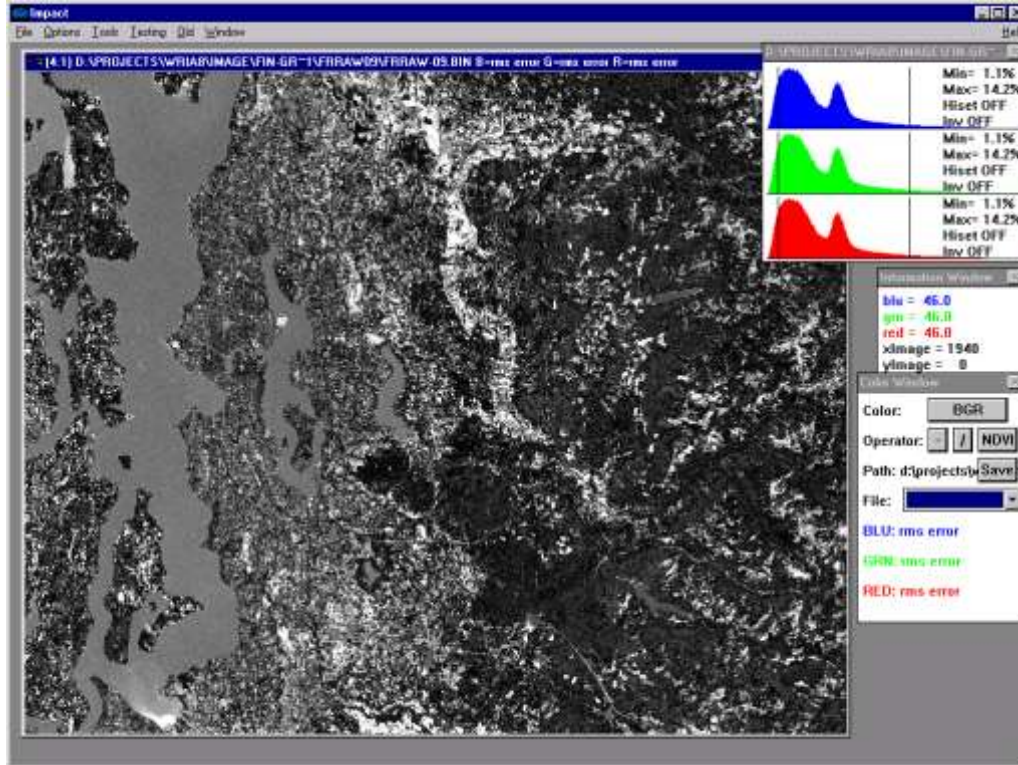
Low/Mid Density Developed model RMS fraction image



The High Density Developed model shows a relatively better fit in dense urban areas than the fit for either Rural/Forest/Agriculture or Low/Mid Density Developed. Inspection of the RMS fraction image from the High Density Developed

model shows lower values (darker pixels) in the urban core areas and higher RMS values in rural areas than either of the other models. This pattern suggested that RMS could be used to indicate which model best explained its composition.

High Density Developed model RMS fraction image. (487k)



### *Model Integration:*

The three models were treated in a hierarchical order by their overall RMS values. Areas with Rural/Forest/Agriculture model RMS values less than 15% retained their endmember fractions for Green Vegetation, Bare Soil, Dry Grass and Shade. Cells with more that 15% RMS in the Rural/Forest/Agriculture model but with less than 15% RMS in the Low/Mid Density Developed model received endmember fractions from the Low/Mid Density Developed model: Green Vegetation, Impervious 1, Dry Grass, and Shade. The remaining pixels without values were those that did not have a good fit with either of the previous two models and were assigned endmember fraction values from the High Density Developed model (Green Vegetation, Impervious 1, Impervious 2, Shade).

### *Post Integration Processing:*

The Shade endmember was included in each mixture model to normalize the effects of texture and variations in illumination caused by topography. To remove the

effects of texture and topography, pixel composition percents were calculated without the raw values of the Shade endmember. The raw endmember values for each pixel was divided by the sum of all endmembers found in the pixel to produce normalized percent fraction images. At this point, the values for Impervious 1 and Impervious 2 were combined into a single Impervious percent value.

The values for Shade were retained and used to help distinguish between pixels of open green vegetation and forest canopy. Cells that had green vegetation percents greater than the total percent of the other endmembers present and had high shade values were identified. Cells that met this criterion and had all eight neighbor cells meet the criterion as well were considered to be forest canopy. This use of spatial association with other forest canopy cells helped exclude individual trees or patches of shaded grass from the set of forest canopy cells. All other green vegetation values not in cells identified as forest canopy were considered to be ' open vegetation' .

During examination of the forest canopy cells, an error in the classification process was observed. Forest canopy known to be composed of conifers commonly contained Impervious endmember percents clustered around 18%. As the areas examined were known to have no rock outcroppings or other paved surfaces, this was attributed to either an inability of the bright green endmember to effectively model the dark green of conifers, or some confusion between non photosynthetic vegetation (bark & dry needles/leaves) and the impervious endmember. To correct for this error, all impervious values less than 20% found in forest canopy pixels were added to the green vegetation endmember.

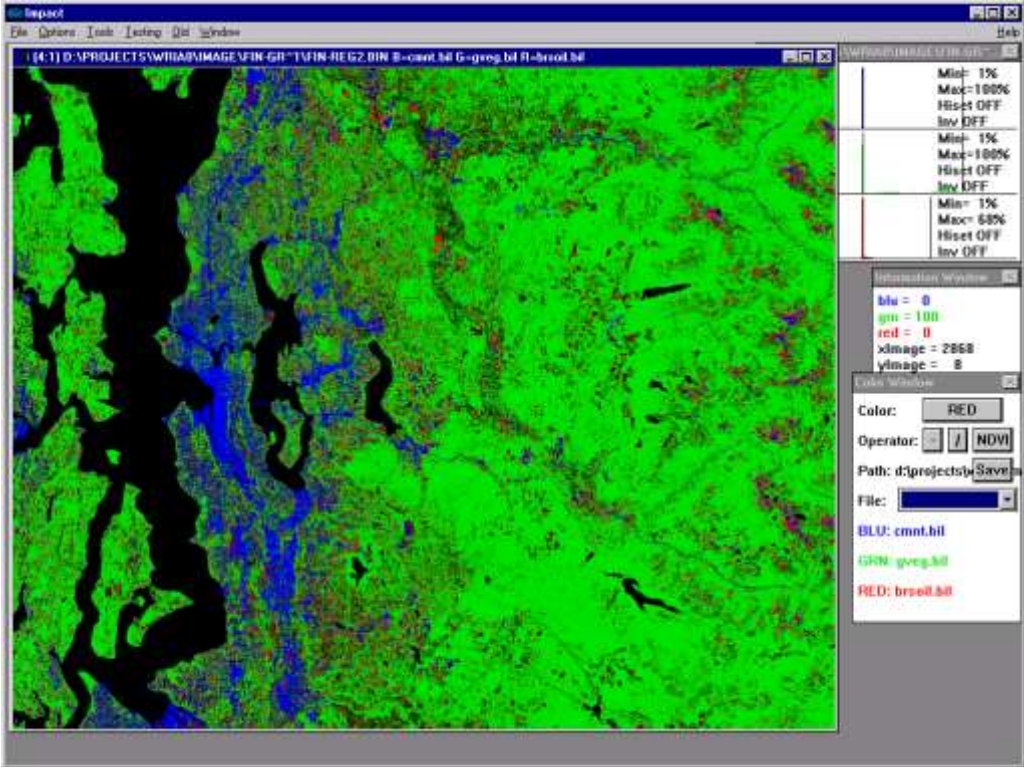
At this point, the analysis results were registered to the USGS 10 meter digital elevation model (DEM). The original image was aligned with the DEM in some areas, but exhibited a varying offsets in others. Registration was performed on SMA results to prevent the introduction of error in pixel spectra from interpolation. The edges of open water bodies, a feature identifiable in both the SMA results and the DEM, were used to measure the degree of offset at eighty points across the analysis area. From these measurements, areas of homogeneous offset were identified and the constituent pixel values shifted together to align with the DEM.

With registration complete, all endmembers from pixels located in open water were assigned a value of zero. Water was not included as an endmember in the SMA and areas of open water often received high impervious percent values after removing the effects of Shade. A vector file delineating the bodies of open water from the USGS 7.5 minute topography quadrangles prepared by the Indian Fisheries Commission was used to mask water pixel values.

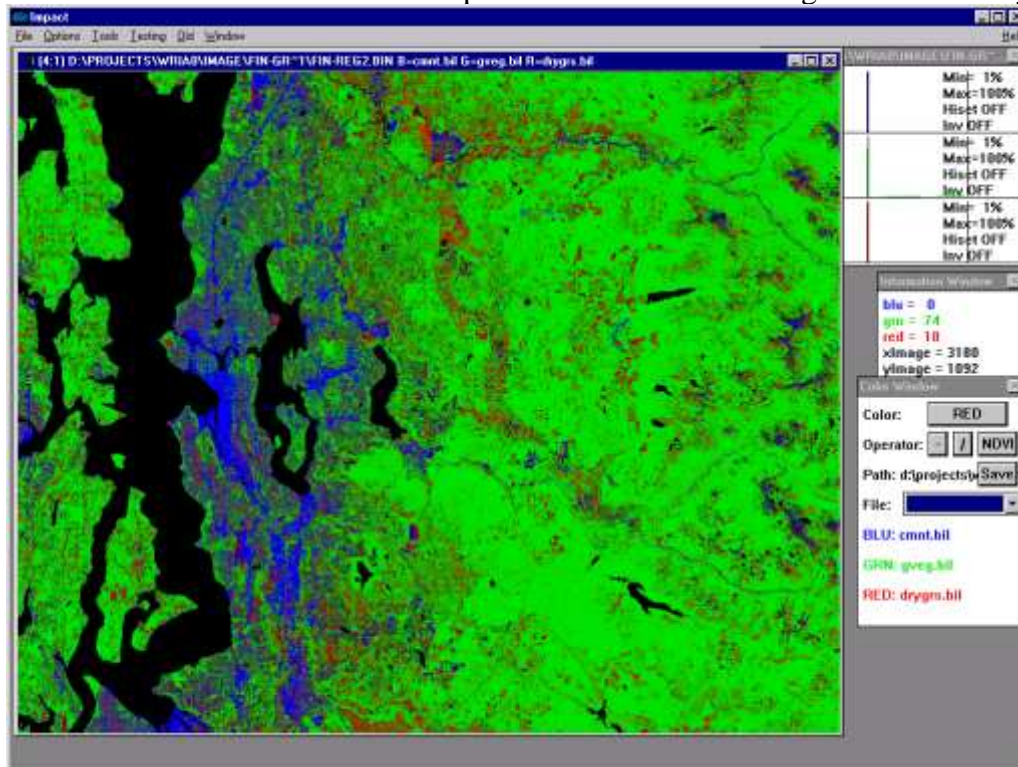


The following links show screen shots from Impact (Software built by the University of Washington Geological Remote Sensing Laboratory). The three screen color guns were each loaded with an endmember fraction image as noted in the link.

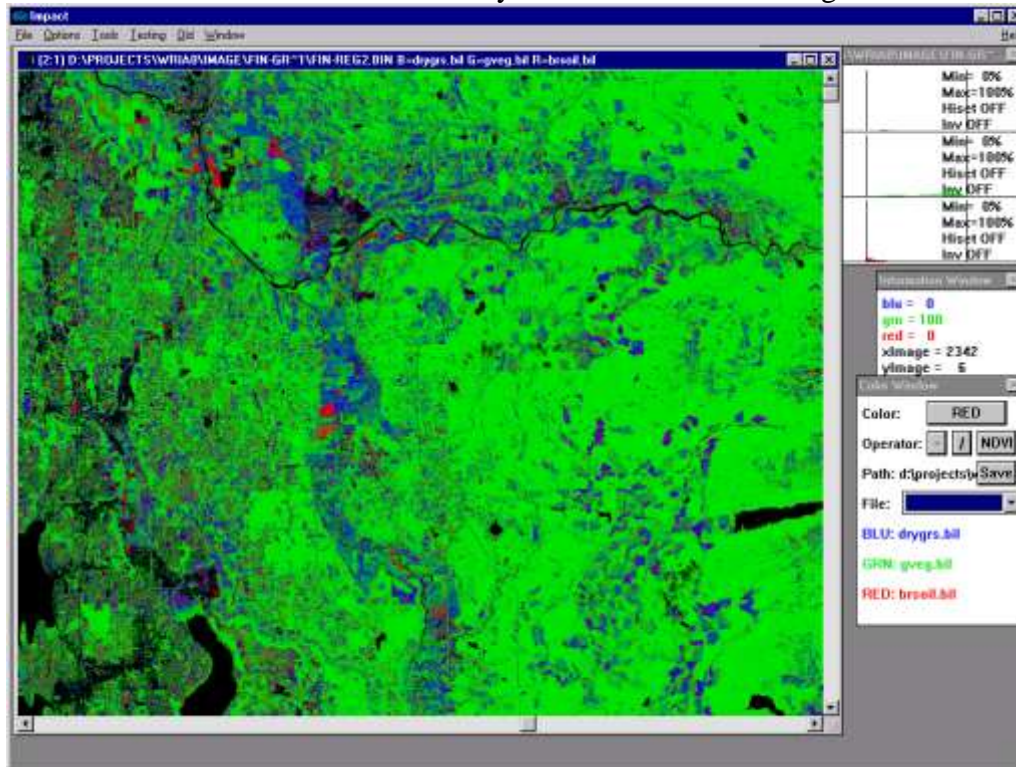
Analysis Results 1 - Full Extent: Blue=Impervious Green=Green Vegetation Red=Bare Soil



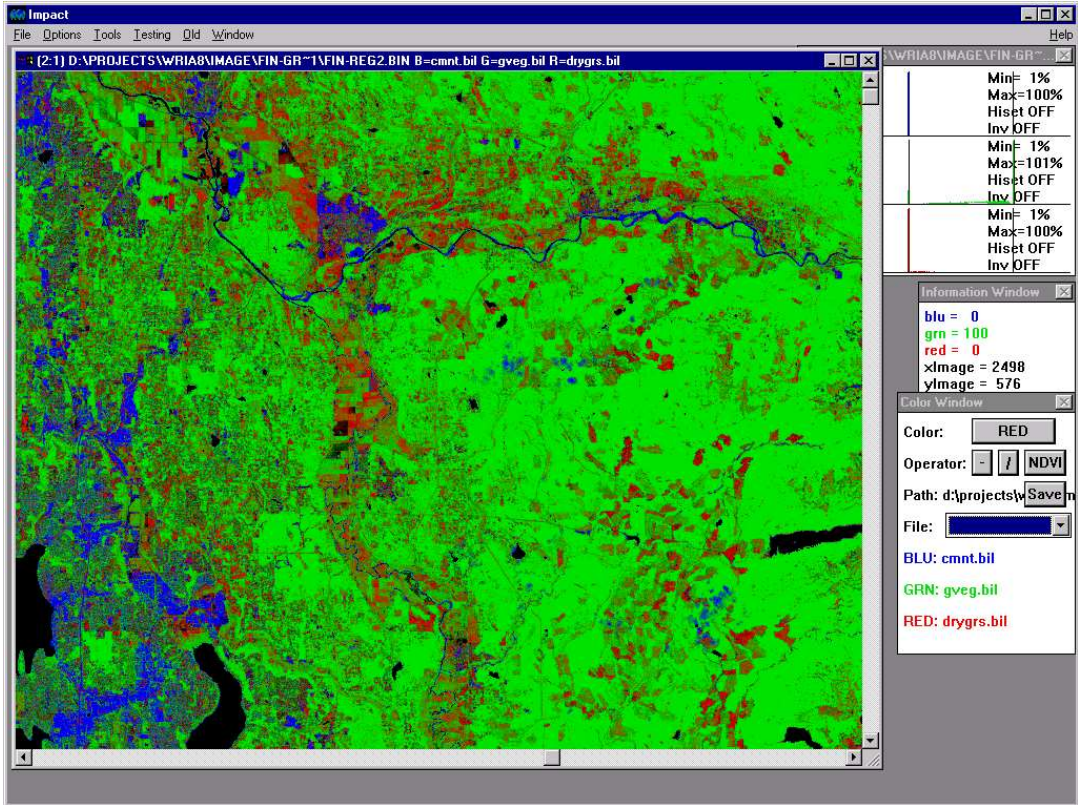
Analysis Results 2 - Full Extent: Blue=Impervious Green=Green Vegetation Red=Dry Grass



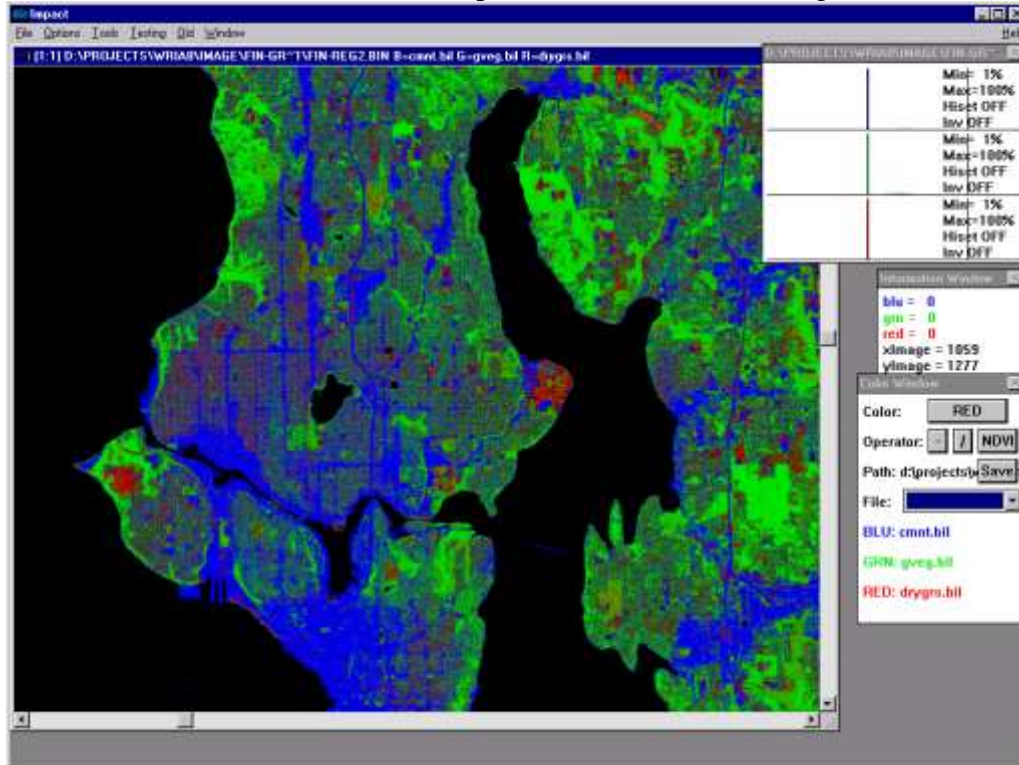
Analysis Results 3 - Monroe-Duval: Blue=Dry Grass Green=Green Vegetation Red=Bare Soil



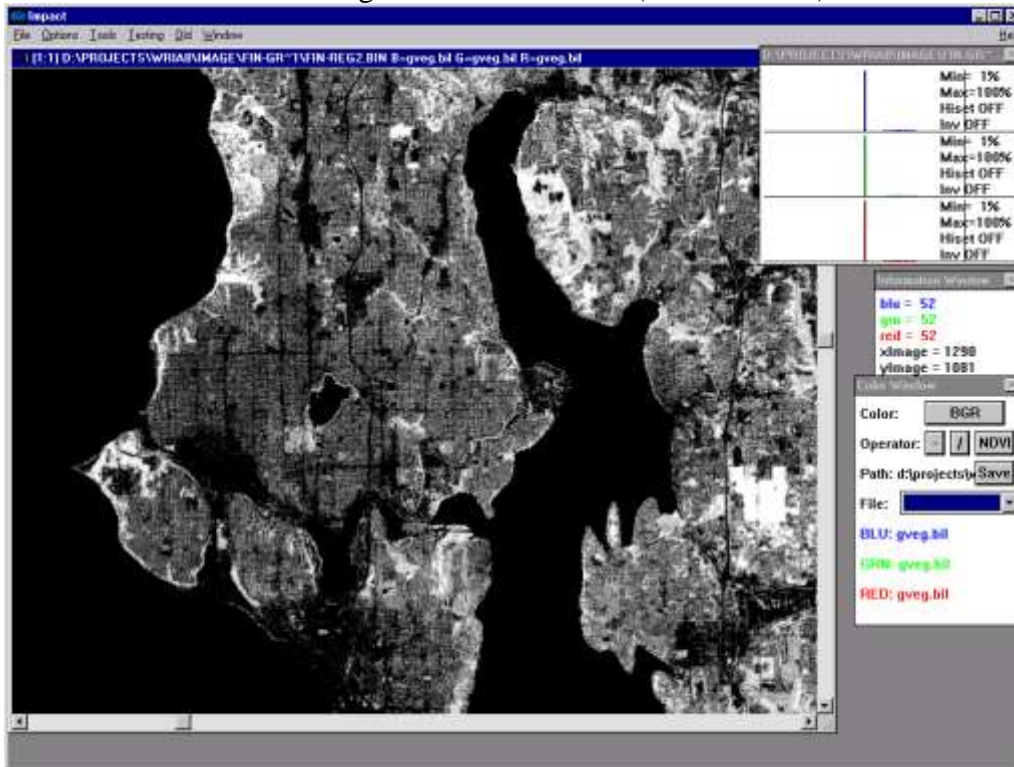
[Analysis Results 4 - Monroe-Duval: Blue=Impervious Green=Green Vegetation Red=Dry Grass](#)



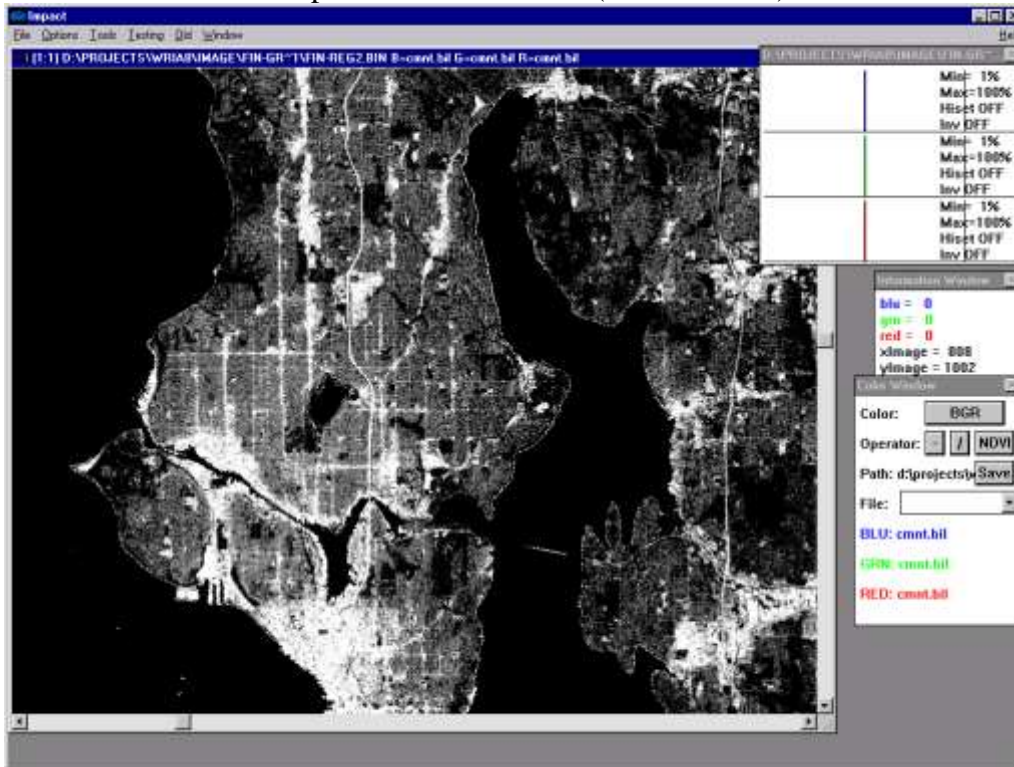
Analysis Results 5 - North Seattle: Blue=Impervious Green=Green Vegetation Red=Dry Grass



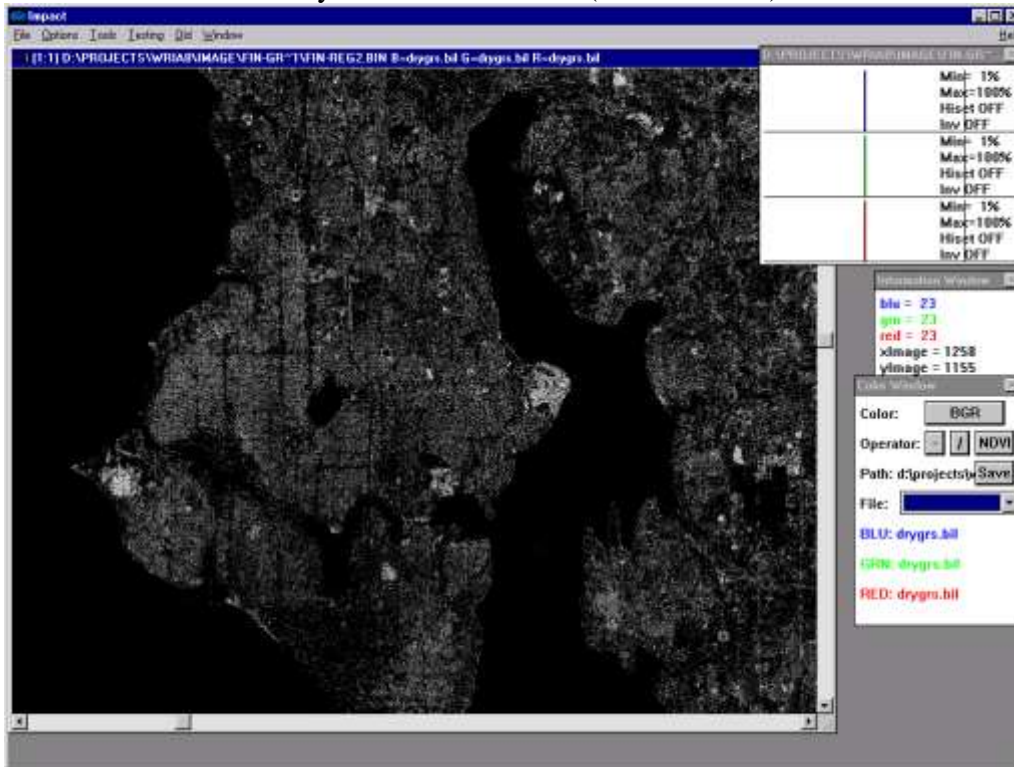
# Green Vegetation Endmember (Monochrome)



# Impervious Endmember (Monochrome)



## Dry Grass Endmember (Monochrome)



### *Testing and Verification:*

One of the most important components in analyzing remotely sensed data is an assessment of accuracy (for a review of methods see Congalton, 1991). While traditional methods of ground truth and accuracy assessment for image classifications may be applied to SMA results, they do not address sub-pixel endmember fractions. Despite this limitation, it is still important to verify the accurate detection of major land cover or land use patterns detected with SMA. The analysis results were compared to digital orthophotos to confirm that the image endmembers selected were indeed identifying the features in the landscape they represent. This is especially apparent in the images of North Seattle where major highway corridors and urban centers appear as blue (impervious) and tree covered drainage ravines are identified as green vegetation. Sand Point and Discovery Park, both with large grassy areas, are identified in red (dry grass) as August 1998 was particularly dry.

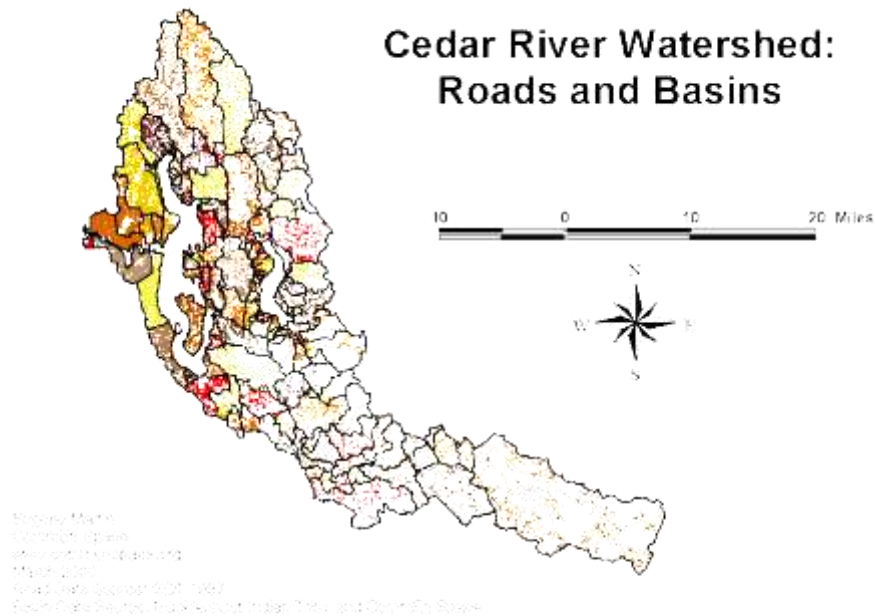
Beyond broad confirmation of endmember detection, confirming individual pixel's endmember percents is far more difficult. The inability to re-create the exact conditions under which the original image was recorded precludes field testing the



components contributing to a particular pixel' s variability (see Sabol et al., 1992). Furthermore, exact registration of the image to coincide with the specific 28.5 meter square portion of the Earth' s surface makes quantification of pixel constituent components difficult. Recognizing these barriers to verifying pixel endmember percents, an alternative approach was adopted to corroborate trends in endmember percents through relationships or proximity to known features in other geographic data sets (see Smith et al., 1990a). Two tests were used to confirm impervious surface detection at different spatial scales: correlation of impervious surface area with road length in sub-watersheds and average impervious area per pixel verses distance to streets and buildings.

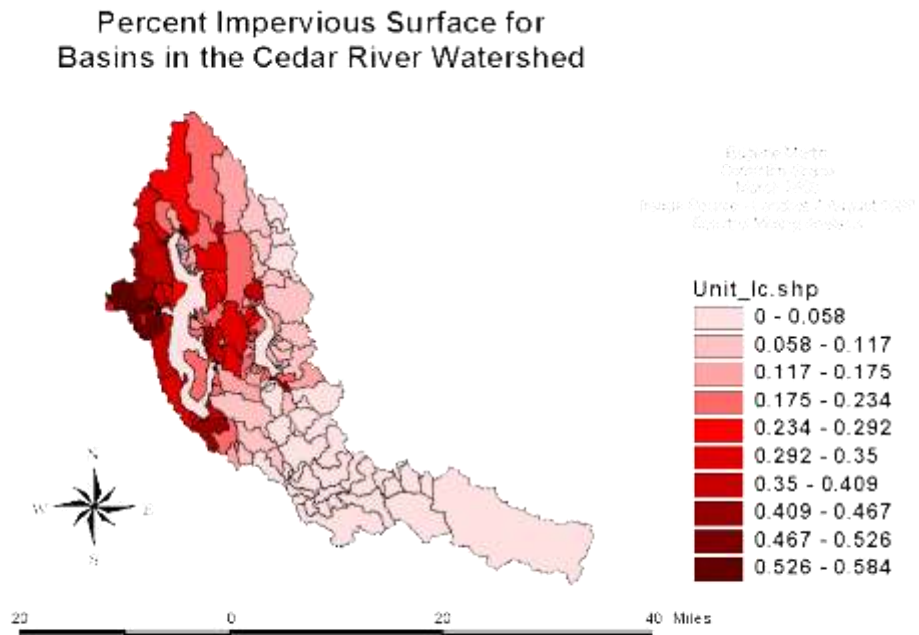
During preparation of the Muckleshoot Indian Tribe' s Chinook Recovery Plan, 158 sub-watershed units of the Cedar River watershed were identified and delineated. The length of road in each sub-watershed unit was calculated using General Data Technology' s 1997 road data set distributed by ESRI with their Street Map software.

Map1: Cedar River Watershed: Roads and Basins



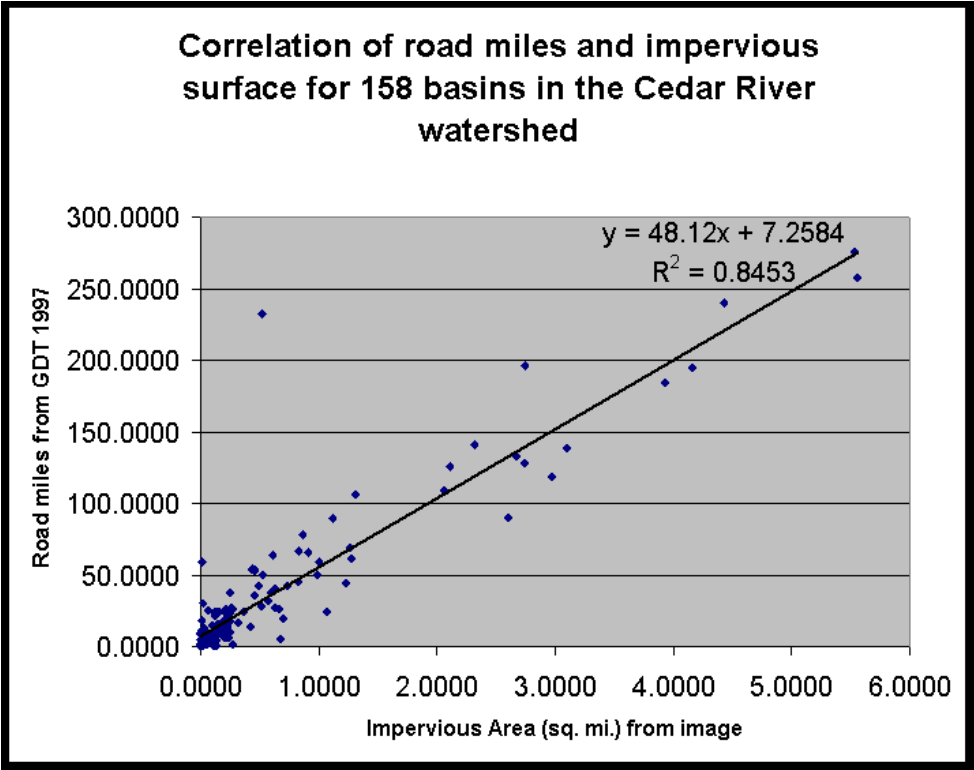
Impervious area from the SMA was calculated by multiplying the impervious endmember percent by pixel area (812.25 square meters) and summing across all pixels in each of the sub-watershed units.

Map2: Percent Impervious Surface for Basins in the Cedar River Watershed



A regression analysis of these two variables indicated a strong positive correlation ( $R^2 = 0.82$ ). The value furthest from the regression line corresponded to the headwaters of the Cedar River where the majority of roads are unpaved logging access roads that in some cases are overshadowed by adjacent trees. While this test does not assess the accuracy of sub-pixel components or position relative to impervious surface, it does indicate that detection of impervious surface at the sub-pixel level has a positive linear association with a feature in the landscape that is known to be impervious.

Figure1: Correlation of road miles and impervious surface for 158 basins in the Cedar River Watershed.



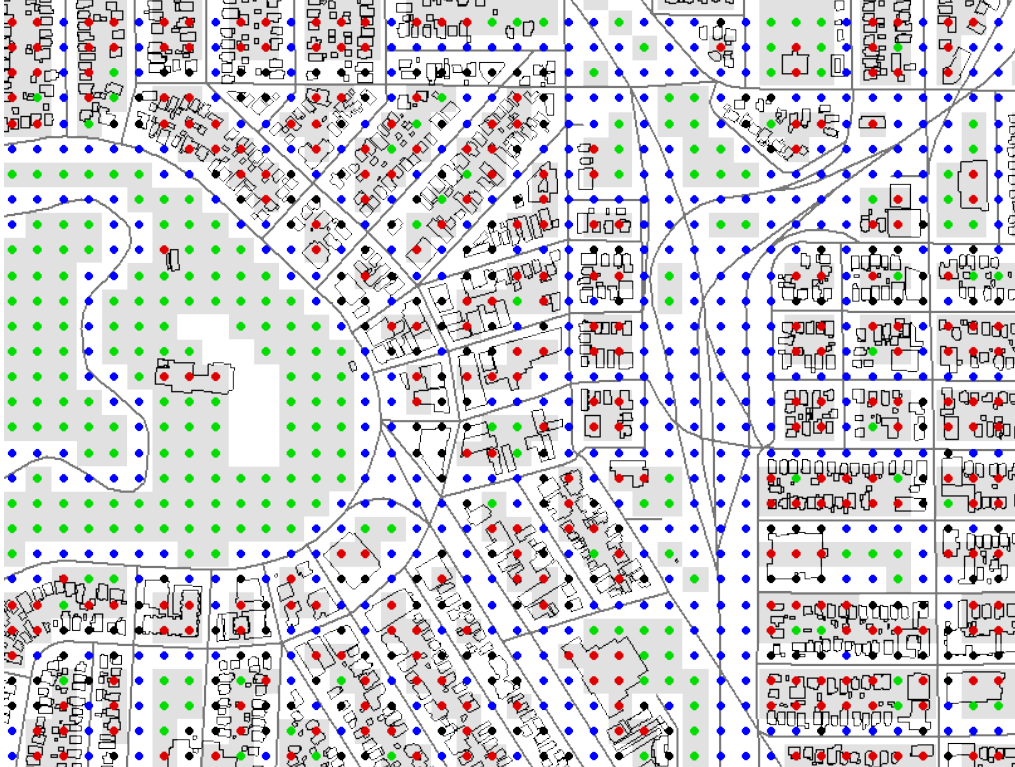
Another test was made to compare pixel impervious surface area to pixel distance from impervious features. A portion of the City of Seattle including the central business district and extending to the north-east was selected for its variety of urban elements: parks, open spaces, residential, highway corridors and downtown core.

Impervious surface cell area test clip: Seattle - Downtown, Lk. Union, Greenlake, U. District



A portion of the City of Seattle geographic information data set for buildings and streets was clipped and projected to register with the image (UTM27 Zone 10 – NAD 27). To exclude the obvious influence of pixels in water bodies (previously masked) and in open areas, only pixels within 100 meters of a road in the City data set were included in the test. After exclusion, 81652 pixels were eligible for testing. The street vectors were converted to a raster with the same resolution and lattice as the image (28.5 meter cells) using the default vector to raster conversion available in Spatial Analyst 1.1. These road pixels were used as a mask to divide the test pixels into two groups. The center points for all the test pixels were derived and evaluated for their distance to building outline polygons from the City’ s data. This measure served to divide the test pixels into two additional categories: pixels with center points within 5 meters of a building and pixels further than 5 meters from a building. The intersection of these two classifications produced four distinct classifications of test pixels based on their proximity to impervious features. Averages and standard deviations for pixel impervious surface area were calculated for each test pixel category:

Impervious surface cell test schematic (close up sample).



Legend:

Thick Gray Line: City of Seattle road vector

Thin gray polygon outlines: City of Seattle building outlines

Blank Space: indicates cells more than 100 Meters from a road or building

● Green: Not a road cell and >5M from a building

● Blue: A road cell and >5M from a building

● Red: Not a road cell and <5M from a building

● Black: A road cell and <5M from a building

Table 2: Test pixel categories and statistics.

	COUNT	AVE. IMP AREA	STDDEV
● Green	20964	231.7906	282.0444
● Blue	26422	392.8923	263.8372
● Red	24608	402.7362	240.0314
● Black	9658	450.9680	243.0476

This test demonstrates a general trend of increasing average impervious surface with proximity to a street and/or building. Also worth noting is the decrease in standard deviation with proximity to buildings and streets.

Using digital geographic information sources to confirm or refute sub pixel content percentages is difficult because registration to the image can only be made to within the distance of half a pixel under ideal conditions. Furthermore, the measurement process that produced the image content and the geographic data are fundamentally different. The City of Seattle data set does not include sidewalks or parking lots, both of which are important contributors to impervious surfaces in urban environments. In locations where this is the case, the image will provide a better measure of impervious surface than the geographic data. Furthermore, there are many places in the test area where trees overshadow buildings and roads which results in disagreement between the data sources. In these locations, the image will underestimate impervious surface and the geographic data will approximate reality. These two sources of variability are believed to account for the high standard deviation values reported in the testing of pixel proximity to impervious features above. The decrease in standard deviation of pixel impervious area with greater proximity to known impervious features suggests that there are fewer gross discrepancies between the two data sources on or about these features confirming detection.

*Directions for Further Development:*

This research has demonstrated the potential of SMA to quantify impervious surfaces in a diverse landscape with an urban component. Despite this success, there are two broad areas where the process can be improved: 1) include more endmembers in a greater variety of mixing models; and 2) refine the testing and verification process. The use of several green vegetation endmembers (grass, deciduous and conifer) and additional impervious surface endmembers (asphalt and tarpaper), would improve both the capacity of the process to detect impervious surfaces and assist the process of verifying results. Reducing the number of endmembers included in each model while increasing the number of models to be integrated would help to improve the use of RMS to indicate which model to use for which pixel. Using pairs of endmembers along with the shade proxy in each mixing model would achieve better detection of the two most important components in each pixel. In this situation, differences in RMS between pixels with a good fit versus a poor fit would be greater permitting better discrimination in which model to assign.

Towards better testing and verification, more accurate and complete geographic data should be developed on specific locations to support the testing of pixel mixtures. Exact measures of the location, type and extent impervious surface and an other major surface components (vegetation, soils, non-photosynthetic vegetation). This model should be developed in three dimensions to permit the assessment of shade

from buildings and trees for the angle of illumination at the time the source image is recorded. These data locations need to have an extent that would cover several pixels (maybe 300 x 300 meters) and be located across a continuum from high density urban to disturbed rural. Building the verification data sets using vector data structures will facilitate projection and geospatial correction to match the coordinate system of the source image.

Finally, as this method produces more detailed information on the nature and distribution of impervious surfaces, the ability of SMA to inform on watershed processes needs to be examined. At this point, the results of this research are being used to assess and compare the conditions of watersheds and their suitability for salmon habitat rehabilitation. With refinements to the methods and calibration, the physically based measurements of features in a landscape produced with SMA will be appropriate inputs for surface water runoff models.

#### *Bibliography:*

Adams, J. B., M. O. Smith, et al. (1986). "Spectral mixture modeling: a new analysis of rock and soil types at the Viking Lander 1 site." *J. Geophys. Res.* **91**(B8): 8098-8112.

Adams, J. B., M. O. Smith, et al. (1989). "Simple models for complex natural surfaces: a strategy for the hyperspectral era of remote sensing." *Proc. IGARSS 1989 Vancouver BC* **1**: 16-21.

Adams, J. B., M. O. Smith, et al. (1993). Imaging spectroscopy: interpretation based on spectral mixture analysis. *Remote Geochemical Analysis: Elemental and Mineralogical Composition*. C. M. Pieters and P. Englert. New York, Cambridge University Press. **7**: 145-166.

Adams, J. B., D. E. Sabol, et al. (1995). "Classification of multispectral images based on fraction of endmembers: application to land-cover change in the Brazillian Amazon." *Remote Sens. Environ.* **52**: 137-154.

Adams, J. B. and M. O. Smith (1996). Changes in Vegetated Landscapes: A Process-Model Approach to Multispectral Remote Sensing. *Remote Sensing for Land Degradation and Desertification Monitoring in the Mediterranean Basin*. D. Peter. Brussels, Commission of the European Countries.

Booth, D. (1991). "Urbanization and the natural drainage system-impacts , solutions and prognoses." *Northwest Environmental Journal***7**(1): 93-118.

Booth, D. and L. Reinelt (1993). Consequences of urbanization on aquatic systems - measured effects, degradation thresholds, and corrective strategies. *Proceedings Watershed '93 A National Conference on Watershed Management*. Alexandria, Virginia: 545-550.

Cochrane, M. A. and C. M. S. Jr (1998). "Linear mixture model classification of burned forests in the Eastern Amazon." *Int. J. Remote Sensing* **19**(17): 3433-3440.

Congalton, R. G. (1990). "A Review of Assessing the Accuracy of Classification of Remotely Sensed Data." *Remote Sens. Environ.***35**: 35-46.

Galli, J. (1991). *Thermal impacts associated with urbanization and stormwater management best management practices*. Washington DC, Metropolitan Washington Council of Governments. Maryland Department of Environment.

Gillespie, A. R., M. O. Smith, et al. (1990). Interpretation of Residual Images: Spectral Mixture Analysis of AVIRIS Images, Owens Valley, California. *Proc. Airborn Sci. Workshop: AVIRIS*. Pasadena California, JPL Publication. **90-54**: 243-270.

Gillespie, A. R., M. O. Smith, et al. (1990). Spectral Mixture Analysis of Multispectral Thermal Infrared Images. *Proc. 2nd Thermal IR Multispectral Scanner (TIMS) Workshop*. Pasadena California, JPL. **90-55**: 57-74.

Horowitz, H. M., R. F. Nalepka, et al. (1971). Estimating the proportions of objects within a single resolution element of a Multispectral Scanner. Ann Arbor, University of Michigan NASA Contract NAS-9-9784.

Roberts, D. A., M. O. Smith, et al. (1990). Isolating Woody Plant Material and Senescent Vegetation from Green Vegetation in AVIRIS Data. *Proc. Airborne Science Workshop: AVIRIS*. Pasadena, California, Jet Propulsion Lab. **90-54**: 42-57.

Sabol, D. E., J. B. Adams, et al. (1992). "Quantitative Subpixel Spectral Detection of Targets in Multispectral Images." *Journal of Geophysical Research* **97**(E2): 2659-2672.

Sabol, D. E., D. A. Roberts, et al. (1993). Mapping and Monitoring Changes in Vegetation Communities of Jasper Ridge, CA Using Spectral Fractions Derived



from AVIRIS Images. *Proc. 4th Annual JPL Airborne Geoscience Workshop*.  
Washington DC, Jet Propulsion Lab.

Sabol, D. E. (1995). Monitoring Land-Use Over Time Using Spectral Mixture Analysis. *Elements of Change 1995*: 79-81.

Schueler, T. (1994). "The Importance of Imperviousness." *Watershed Protection Techniques* `1(3).

Shaver, E. J., C. G. Maxted, et al. (1994). Watershed protection using an integrated approach. *Stormwater NPDES Related Monitoring Needs.*, Engineering Foundation. American Society of Civil Engineers.

Smith, M. O., S. L. Ustin, et al. (1990). "Vegetation in Deserts: I. A Regional Measure of Abundance from Multispectral Images." *Remote Sens Environ.* **31**: 1-26.

Smith, M. O., S. L. Ustin, et al. (1990). "Vegetation in Deserts: II. Environmental Influences on Regional Abundance." *Remote Sens. Environ.* **29**: 27-52.

Tompkins, S., J. F. Mustard, et al. (1997). "Optimization of Endmembers for Spectral Mixing Analysis." *Remote Sens. Environ.* **59**: 472-489.

Ustin, S. L., M. O. Smith, et al. (1993). Remote Sensing of Ecological Processes: A Strategy for Developing and Testing Ecological Models Using Spectral Mixing Analysis. *Scaling Physiological Processes: Leaf to Globe*, Academic Press, Inc.: 339-357.

Wessman, C. A., C. A. Bateson, et al. (1997). "Detecting Fire and Grazing Patterns in Tallgrass Prairie Using Spectral Mixing Analysis." *Environmental Applications* **7**(2): 493-511.

Copyright © 1999-2001 CommEn Space.

Except where otherwise indicated, all materials on this site are protected by applicable U.S. and international copyright laws.